Full Paper

INVESTIGATION OF MICRO-PITS FORMATION ON BILLET SURFACES IN PLANE STRAIN EXTRUSION

I. M. Izhan, S. Syahrullail*, S. Y. Yong, M. A. Nurul

Faculty of Mechanical Engineering, Universiti Teknologi Malaysia, 81310 UTM Johor Bahru, Johor, Malaysia

Graphical abstract
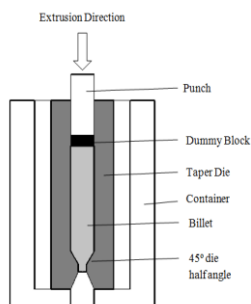
Abstract

Extrusion is a process of pushing a material through a die to yield a desired cross-section product. The application of surface texture has become well known for enhancing tribological performance. In this research, the effect of micro-pits embedded on a work piece lubricated with vegetable oil using plain strain extrusion were studied and compared with those seen with mineral-based oil lubricant. The experiments were conducted at room temperature (around 27℃). A taper die with a 60 die half-angle, with micro-pits array, was prepared. Test lubricants used were paraffinic mineral oil (PMO) VG460 and VG95 and refined, bleached and deodorized (RBD) palm stearin. The results were analysed to determine the extrusion load and the billet's surface roughness and plastic deformation. RBD palm stearin was recorded as having the highest extrusion load (83.15 kN).

Keywords: Vegetable oil, cold extrusion, paraffinic mineral oil, RBD Palm stearin, surface roughness

1.0 INTRODUCTION

Extrusion is a process used to push a material through a die to yield a desired cross-section product. Generally, there are two types of extrusion: cold and hot. Some of the advantages of this process are the low material consumption, high dimensional accuracy and surface quality (Syahrullail *et al*., 2013a; Hosseini *et al*., 2015). However, since extrusion is a bulk deformation process, it is known that die tools and materials are subjected to high compression and shear load, leading to tool damage and unsatisfactory product quality (Chaudhari *et al*., 2012).

Metal-forming lubricants are applied to the interface of die tools and materials to reduce friction and wear; the most commonly used are mineral- or synthetic-based lubricants. Chiong *et al*. (2012) stated that due to the need to prevent further pollution of the environment, eco-friendlier materials are being used as alternative lubricants. Abdulquadir *et al*. (2008) performed a study using vegetable oils as metal-forming lubricants, finding that some of them

performed adequately. Hafis *et al*. (2013) stated that Malaysia is the main producer and exporter of palm oil globally; one of the palm oil products, RBD palm stearin, was proven by Syahrullail *et al*. (2011a; 2011b) to produce a lower working load in the extrusion of a billet than some of the mineral-based oils.

For years, the application of surface texture has been well known for enhancing tribological performances; it helps to reduce load capacity and the friction coefficient between surfaces. Surface textures are also known for having micro-pits, oil pockets, dimples and cavities. Micro-pits act as miniature reservoirs that trap lubricant, which then escape and form micro-hydrodynamic lubrication film that helps to separate two interfaces. Oil pockets also help to trap wear debris (Koszela *et al*., 2007; Lo and Wilson, 1999). Nowadays, there have been some instances of the mechanical industry using micro-pits as an alternative for reducing wear and friction; however, the mechanism of micro-pits is not completely practical in metal formation due to a lack of understanding of individual parameters' influence on the tribological system (Bay *et al*., 2002). Etsion

(2005) stated that the optimisation of texturing is normally done on a trial and error basis. There is also scant information about the impact of micro-pits on the extrusion process. Accordingly, the purpose of this research is to assess the influence of a textured taper die on the performance of palm stearin during plain strain extrusion.

2.0 MATERIALS AND METHODS

2.1 Experimental Apparatus

Plain strain extrusion was the main method chosen for this study. The arrangement of the apparatus is shown in Figure 1. The workpiece, also known as a billet, was the main component; it was extruded between two taper dies and covered with a container wall, as shown in Figure 1. Aluminium A1100 was chosen as the material for the billet. A plate of aluminium was cut using an electric NC wire-cutting machine to form the required billet shape, as shown in Figure 2. For each experiment, two billets were merged together as one element and one side of the billets' stacked surfaces was a square pattern gridline, inscribed using a marking machine for the purpose of observing plasticity flow after the extrusion process. The gridlines formed v-shaped grooves 0.5 mm deep and 0.2 mm wide at intervals of 1.0 mm. The billet underwent an annealing process before each experiment. The observation plane was not affected by the frictional constraint from the parallel side walls.
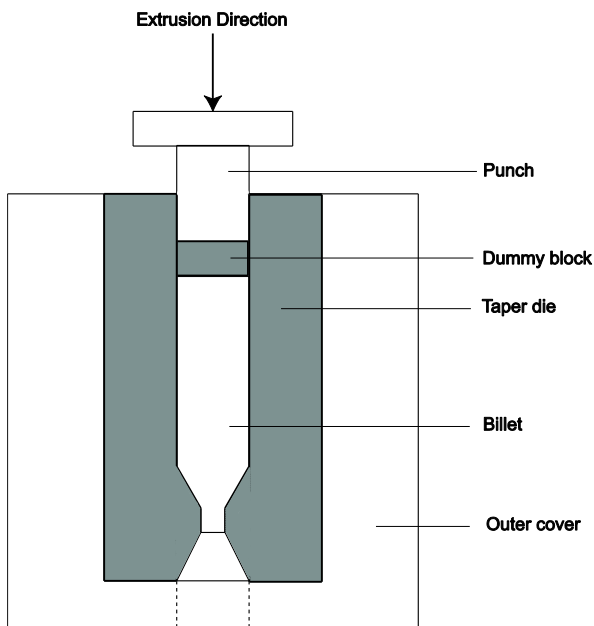

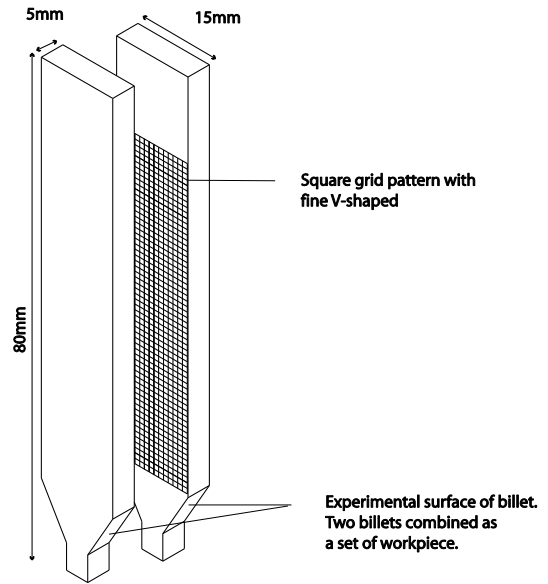**Figure 1** Schematic diagram of the extrusion apparatus

Figure 2 Schematic sketch for the billet

2.2 Taper Die

The taper dies used in this experiment were made of tool steel JIS SKD11 with a 60 degree die half angle. A schematic sketch of a taper die without micro-pits is shown in Figure 3. The taper area was textured using a marking machine; Figure 4 shows a schematic sketch of a taper die with micro-pits and its dimensions. Micro-pits were spherically shaped with a diameter of 0.2 mm and depth of 0.03 mm, as shown in Figure 4. Distance between pits was 1.0mm. The textured taper dies were hardened before use.
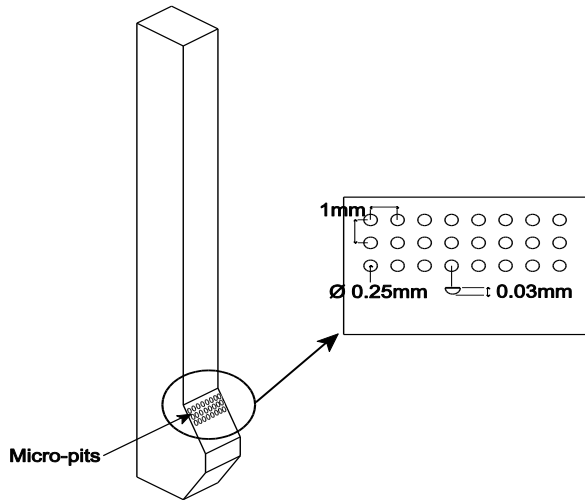

Figure 3 Taper die without micro-pits

Figure 4 Drawing of taper die with micro-pits

2.3 Test Lubricants

The test lubricants used were paraffinic mineral oil (PMO) VG460, paraffinic mineral oil (PMO) VG95 and refined, bleached and deodorised (RBD) palm stearin. Test lubricants were applied to the surface of taper dies just before the extrusion process in amounts of 15 mg. Table 1 shows the properties of PMO VG460, PMO VG95 and RBD palm stearin.

Table 1 Kinematic viscosity and viscosity index of test lubricants

Parameter	RBD Palm Stearin	VG460	VG95
Kinematic Viscosity at ambient T (mm^2/s)	48.29	1374.60	249.95
Kinematic Viscosity at 40°c (mm^2/s)	38.01	411.30	71.75
Kinematic Viscosity at 100°c (mm^2/s)	8.56	28.10	13.4
Viscosity Index	171	95	192

2.4 Experimental Procedure

The components of the plain strain extrusion apparatus were properly assembled and rigidly placed on a hydraulic pressing machine, as shown in Figure 5. The apparatus was grouped into the confinement fixture and placed on the pressing machine. The extrusion load, displacement data and extrusion time were recorded using PME assistant software; the experiments were implemented at room temperature. The billet was constantly pressed and was stopped when the piston stroke reached 35 mm, at which point the extrusion load

and speed held constant values. The stacked billets were dismantled from the extrusion apparatus after the process and separated for the purpose of surface roughness and metal flow analysis. The taper dies were cleaned using acetone to ensure there were no particles trapped on the surface. Experiments were executed three times for each condition to obtain optimum results.
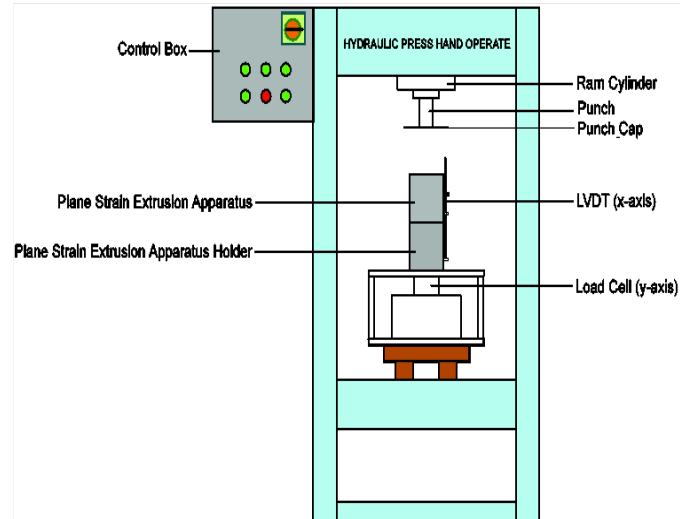

Figure 5 Schematic sketch of hydraulic pressing machine

2.5 Visioplasticity Method

The parallel lines to the direction of extrusion in grid lines on the observation plane of plastic flow of a billet become curved lines and signify the plastic flow lines in the steady state extrusion condition. The schematic diagram of the x-y orthogonal coordinates system was exhibited in Figure 6. The equations below were used in the analyses of the deformation condition. Since the analytical calculation procedure was explained in earlier publications, it is thus omitted here (Syahrullail *et al.*, 2013b).

Flow function:
$$\varphi_i = X_i |V_o| \tag{1}$$

Velocity component (velocity in the x-direction: u, velocity in the y-direction: v):

$$u = \frac{\partial \varphi}{\partial Y}, v = -\frac{\partial \varphi}{\partial X} \tag{2}$$
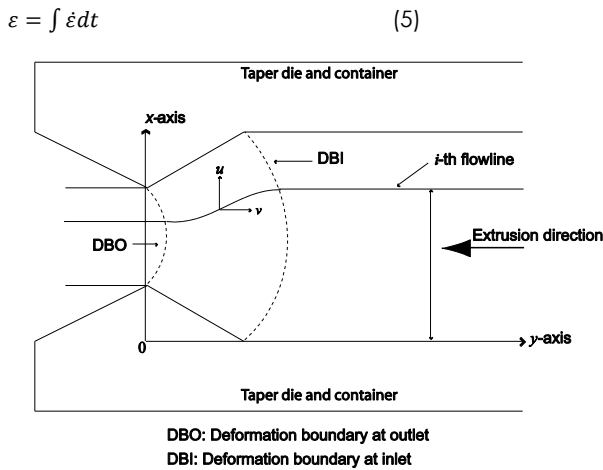
Strain rate component (s^{-1}):

$$\dot{\varepsilon}_X = \frac{\partial u}{\partial X}, \dot{\varepsilon}_Y = \frac{\partial v}{\partial Y}, \dot{\gamma}_{XY} = \frac{\partial u}{\partial Y} + \frac{\partial v}{\partial X} \tag{3}$$

The effective strain rate (s^{-1}):

$$\dot{\epsilon} = \frac{2}{3}\sqrt{3\dot{\varepsilon}_X^2 + \frac{3}{4}\gamma_{XY}^2} \tag{4}$$

The effective strain (time integration value of the effective strain rate along the flow line):

$$\varepsilon = \int \dot{\varepsilon}\,dt \qquad\qquad (5)$$

**Figure 6** The schematic diagram of the x-y orthogonal coordinates system

3.0 RESULTS AND DISCUSSION

3.1 Extrusion Load

Figure 7 shows a plotted graph of extrusion load vs piston stroke. The extrusion process stopped at the piston stroke of 35 mm. As shown by the figure, the extrusion load of three curves increased drastically due to deformation of the work-piece. As it reached plastic deformation stage around 20 mm, the changes of loads were constant until the extrusion process ended at 35mm. In the graph, the billet with PMO VG460 has the lowest extrusion load (43 kN), followed by PMO VG95 (62.16 kN). The process that used RBD palm stearin shows the highest forming load, 83.15 kN.

   PMO VG460 and PMO VG95 demonstrated their aptitude as extrusion lubricants, due to their high viscosity and moderate flowability. During extrusion, lubricants trapped in the micro-pits were able to escape in order to form micro-hydrodynamic lubrication films by separating taper die-billet interfaces. Consequently, less metal-to-metal contact led to reduced friction between surfaces and resulted in a lower extrusion load. RBD palm stearin remained in semi-solid form at room temperature; it easily became stuck inside micro-pits due to its poor flowability. As deformation occurred, micro-pits failed to function in terms of providing a lift to interfaces. The depletion of lubricants caused friction, and thereby the extrusion load, to increase.
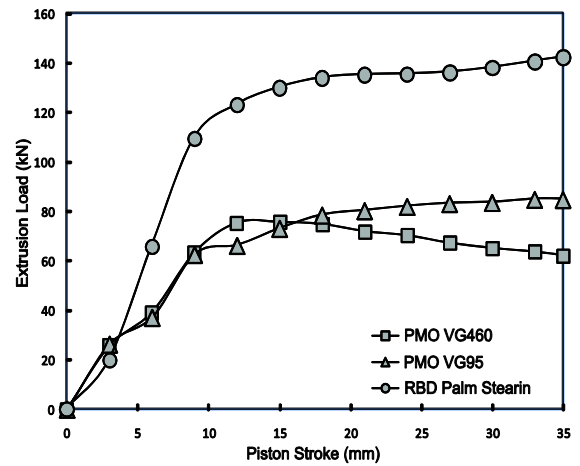
Figure 7 Extrusion load against piston stroke curves

3.2 Surface Roughness Analysis

For the study, the measurement of arithmetic surface roughness, Ra, carried out along the experimental surface of the work-piece, was observed to be (X = 0 mm to X = 12 mm). The experimental surface was the surface where the contact between the taper die and billet was observed. This region is also called the deformation region, as it is where the billet starts to deform during the extrusion process. The product region (X = -2 to X = -6) is the region where the final form of the billet is produced. The direction of the measurement of surface roughness is directly perpendicular to the direction of extrusion. The result of surface roughness in our study is shown in Figure 8.

   As shown in this Figure 8, the billet lubricated with RBD palm stearin had the roughest surface at the deformation region, while the billet extruded with PMO VG460 had the lowest surface roughness overall. This is because PMO VG460 has high viscosity, enabling it to form a thick layer of lubrication film. This helps to reduce metal-to-metal contact between the taper die and billet surface. Therefore, lower friction produces a better billet surface. Having said this, although PMO VG95 has lower viscosity than PMO VG460, micro-pits help to reduce metal-to-metal contact by providing micro-hydrodynamic lubrication film to the interfaces.

   RBD palm stearin can easily get stuck in micro-pits due to its semi-solid form at room temperature. Micro-pits are unable to supply sufficient lubricants to the interfaces; As a result, high friction during deformation caused a rougher billet surface in our study.
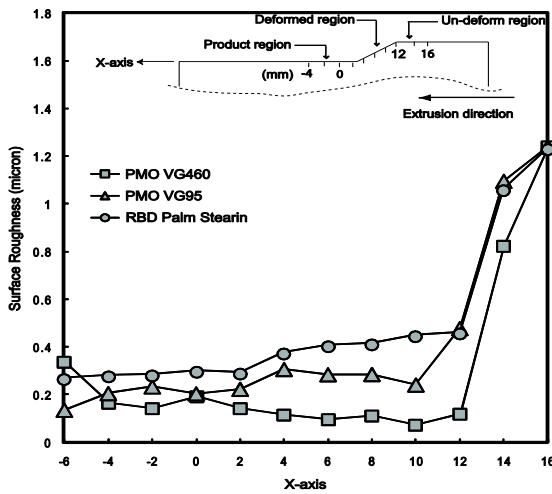
Figure 8 Surface roughnesses, Ra, of the billet's surface

Figure 9 Coordinates used to measure flow angle at billet's surface

3.3 Flow Angle

Figure 9 depicts the coordinates used to measure the inclination of gridlines near to the taper die. The taper die surface was chosen as the deformation zone of the billet positioned in this area. Based on the inclination degree of gridlines, the frictional condition increases as the inclination degree decreases.

Figure 10 shows the gridline inclination distribution on the billet sliding area. The inclination degree was high at the inlet of the deformation area and decreased towards the exit of the deformation area, due to the increment of the extrusion ratio. Deformation occurred around X = 13 mm and ended at X = 3 mm. The flow angles of PMO VG460 were larger compared to those of RBD palm stearin. A higher frictional constraint leads to a smaller flow angle. PMO VG460 has a high flowability and is able to flow out from micro-pits and form lubrication film, therefore it has lower friction and a reduced extrusion load. Meanwhile, RBD palm stearin has a smaller inclination angle due to high friction on the taper die-billet interfaces. As mentioned above, RBD palm stearin has a semi-solid form at room temperature; it does not flow out from micro-pits to act as a secondary lubrication film. As a result, the friction between the tool and work-piece surfaces is higher, leading to a greater forming load.
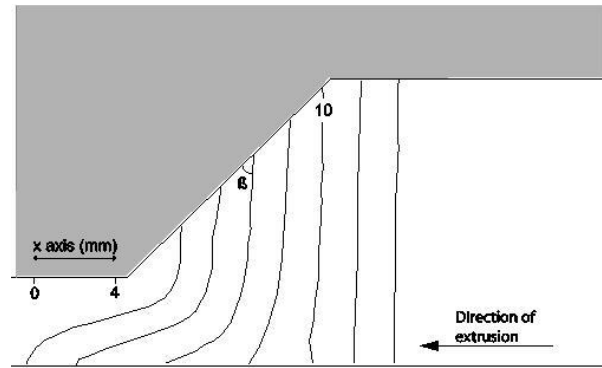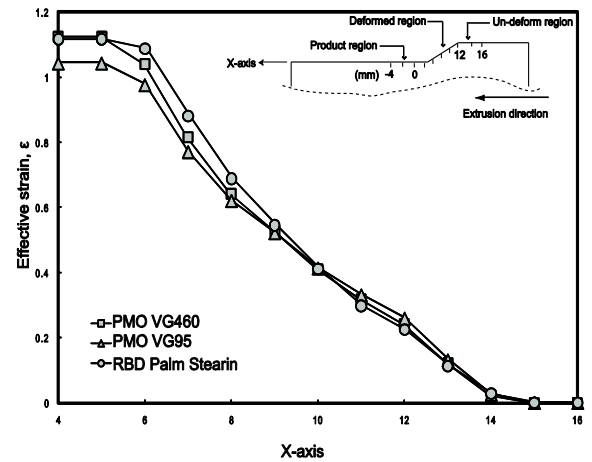

Figure 10 Flow angle against X-axis

3.4 Resultant Relative Velocity

The distribution of resultant relative velocity along the experimental surface is shown in Figure 11. The velocity is the sum of two or more velocity vectors calculated using the visioplasticity method (Syahrullail *et al.*, 2013b).

As shown in Figure 11, a similar pattern of relative velocity was recorded for all experimental conditions. During the deformation stages of the billet, the billet extruded with RBD palm stearin produces the lowest relative velocity. RBD palm stearin could not be stored in micro-pits so was unable to provide lift to separate the taper die and billet, leading to higher friction and lower sliding velocity.

3.5 Effective Strain

Figure 12 exhibits the effective strain for all experimental conditions. It is shown that all the effective strain values increased at the product region as compared to the inlet. The billet extruded with RBD palm stearin showed a higher effective strain at the outlet, compared to PMO VG460 and PMO VG95.
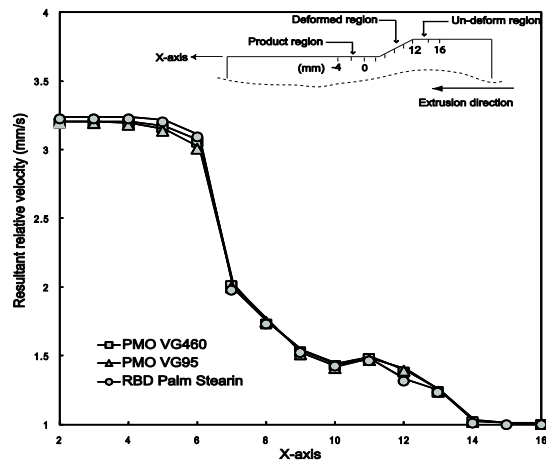
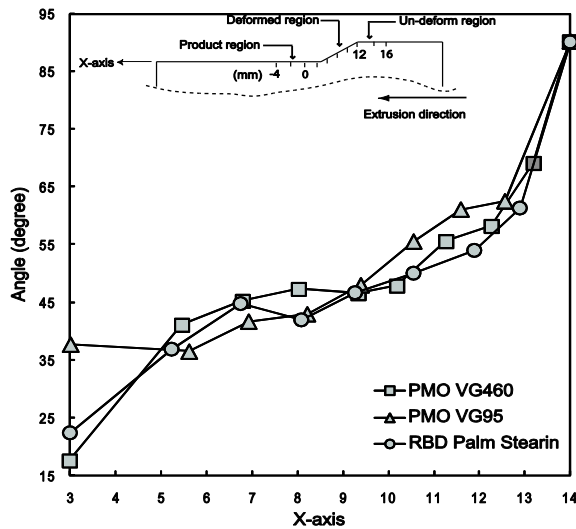**Figure 11** Resultant relative velocity against X-axis

Figure 12 Effective strain against X-axis

4.0 CONCLUSION

An experiment to investigate the influences of textured taper dies on the performance of RBD palm stearin during plain strain extrusion was carried out. The results with RBD palm stearin were compared to those of PMO VG460 and PMO VG95. It was found that:

1. RBD palm stearin produced the highest extrusion load compared to both mineral oils.
2. RBD palm stearin produced the highest value of arithmetic surface roughness, Ra subsequently increase friction between tools.
3. Regarding flow angle, RBD palm stearin had a smaller inclination angle due to high friction at the experimental surface.
4. PMO VG460 had the highest resultant relative velocity.

5. The effective strain obtained lubricated with all tested lubricants higher at the work-piece outlet, compared to the work-piece inlet of the deformation region.

References

[1]   Manabu Wakuda, Yukihiko Yamauchi, Shuzo Kanzaki, Yoshiteru Yasuda. 2003. Effect Of Surface Texturing On Friction Reduction Between Ceramic And Steel Materials Under Lubricated Sliding Contact. *Wear*. 254: 356-363.
[2]   Hafis, S. M., Ridzuan, M. J. M., Farahana, R. N., Ayob, A., Syahrullail, S. 2013. Paraffinic Mineral Oil Lubrication For Cold Forward Extrusion: Effect Of Lubricant Quantity And Friction. *Tribology International*. 60: 111-115.
[3]   Chiong Ing, T., Rafiq, A. K. M., Azli, Y., Syahrullail, S. 2012. Tribological Behaviour Of Refined Bleached And Deodorized Palm Olein In Different Loads Using A Four-Ball Tribotester. *Scientia Iranica*. 19(6): 1487-1492.
[4]   Syahrullail, S., Azwadi, C. S. N., Ing, T. C. 2011. The Metal Flow Evaluation Of Billet Extruded With RBD Palm Stearin. *International Review of Mechanical Engineering*. 5(1): 21-27.
[5]   A. Borghi, E. Gualtieri, D. Marchetto, L. Moretti, S. Valeri. 2008. Tribological Effects Of Surface Texturing On Nitriding Steel For High Performance Engine Applications. *Wear*. 265: 1046-1051.
[6]   Andriy Kovalchenko, Oyelayo Ajayi, Ali Erdemir, George Fenske, Izhak Etsion. 2005. The Effect Of Laser Surface Texturing On Transitions In Lubrication Regimes During Unidirectional Sliding Contact. *Tribology International*. 38: 219-225.
[7]   Dangsheng Xiong, Yongkun Qin, Jianliang Li, Yi Wan, Rajneesh Tyagi. Tribological Properties Of PTFE/Laser Surface Textured Stainless Steel Under Starved Oil Lubrication. Tribology International.
[8]   Stachowiak, G. W., Batchelor, A. W. 2005. *Engineering Tribology*. Elsevier Butterworth Heinemann.
[9]   Bowden, F. P., Tabor, D. 2001. *The Friction And Lubrication Of Solids*. Oxford Classic Series, Oxford University Press.
[10] Syahrullail, S., Nakanishi, K., Kamitani, S. 2005. Investigation Of The Effects Of Frictional Constraint With Application Of Palm Olein Oil Lubricant And Paraffin Mineral Oil Lubricant On Plastic Deformation By Plane Strain Extrusion. *Journal of Japanese Society of Tribologists*. 50(12): 55-63.
[11] Wei Tang, Yuankai Zhou, Hua Zhu, Haifeng Yang. 2013. The Effect Of Surface Texturing On Reducing The Friction And Wear Of Steel Under Lubricated Sliding Contact. *Applied Surface Science*. 273: 199-204.
[12] Taposh Roy, Dipankar Choudhury, Azuddin Bin Mamat, Belinda Pingguan-Murphy. Fabrication and Characterization Of Micro-Dimple Array On Al2O3 Surfaces By Using A Micro-Tooling.
[13] Maleque, M. A., Masjuki, H. H., Haseeb, A. S. M. A. 2000. Effect Of Mechanical Factors On Tribological Properties Of Palm Oil Methyl Ester Blended Lubricant. *Wear*. 239: 117-25.

[14] Mahdavian, S. M. 1982. A Refined Analytical Model For Hydrodynamic Lubrication Of Cold Extrusion And Its Comparison With Experiment. *Journal Of Lubrication Technology*. 104: 46-52.